International Journal of Advanced Engineering Research and Science (IJAERS)
Peer-Reviewed Journal
ISSN: 2349-6495(P) | 2456-1908(O)
Vol-10, Issue-11; Nov, 2023
Journal Home Page Available: https://ijaers.com/
Article DOI:https://dx.doi.org/10.22161/ijaers.1011.4

Adsorption of Ce^{3+} ions using a one-dimensional nanomaterial with natural halloysite-kaolinite dual components

Thao Le Thi Phuong[1,2,3,*], Thoa Nguyen Thi Kim[1,2,3], Duyen Le Thi[1,2,3]

[1] Chemistry Department, Faculty of Basic Science, Hanoi University of Mining and Geology, 18 Vien st., Hanoi, Vietnam
[2] Center for Excellence in Analysis and Experiment, Hanoi University of Mining and Geology, 18 Vien st., Hanoi, Vietnam
[3] BSASD research group, Faculty of Basic Science, Hanoi University of Mining and Geology, 18 Vien st., Hanoi, Vietnam
*Email: lethiphuongthao@humg.edu.vn

Received: 25 Sep 2023,

Receive in revised form: 01 Nov 2023,

Accepted: 08 Nov 2023,

Available online: 15 Nov 2023

***Keywords*— Adsorption, one-dimensional nanomaterial, halloysite, kaolinite, Ce^{3+} ions.**

***Abstract*—** *Rare earth elements are widely used in many technological domains, including reactants, alloying elements, catalysts, batteries, superconductors, etc., because of their unique electro-optical properties. Recovery and separation of rare earth elements are particularly crucial due to the steadily rising demand, as they can enhance scarce resources and reduce radiation-related waste disposal harm. Reports about the harmful effects of rare earth elements on microbes, plants, and animals have become increasingly common in recent years. More dangerously, residues from rare earth elements can build up in the human body through ingestion or digestion in the food chain. Finding a practical and affordable way to use rare earth elements or remove them from our surroundings is therefore essential. To extract these elements, halloysite is processed using a straightforward chemical procedure to produce rare earth metal ion adsorbent materials. The Halloysite that has been processed has a rod-shaped, one-dimensional nanomorphology. Halloysite-kaolinite is the two-phase version of the adsorbent material. The strong adsorption capacity of halloysite for Ce^{3+} is demonstrated by research findings. Halloysite adsorbs Ce^{3+} using the monolayer physical adsorption model and the pseudo-second-order adsorption kinetic equation.*

I. INTRODUCTION

Due to their unique electro-optical properties, rare earth elements are widely used in many technological fields, such as reactants, alloying elements, catalysts, batteries, superconductors, etc [1-5]. Continuously increasing demand makes rare earth element recovery and separation especially important, which can improve limited resources and minimize damage caused by waste disposal caused by radiation. In recent years, there have been more and more reports on the toxic effects of rare earth elements on bacteria, plants, and animals. More seriously, when rare earth elements are inhaled or digested in the food chain, residues can accumulate in the human body. Therefore, it is necessary to find an effective and economical method to exploit or remove rare earth elements from our living environment [5].

As an abundantly available and low-cost natural clay mineral, halloysite has the distinctive morphology of hollow one-dimensional nanotubes, whose walls consist of unit layers with one tetrahedral layer (SiO_4) and one octahedral layer (AlO_6). The outer diameter of halloysite nanotubes is about 50-150 nm, and their length is about 200-1000 nm. High specific surface area, adsorption capacity, physicochemical properties, availability, cost, and

environmental advantages make natural halloysites attractive for many applications [6-9]. Similarly, kaolinite is a bifacial alumino silicate layered clay of the kaolin group comprising octahedral $Al(OH)_3$ and tetrahedral SiO_4. Kaolinite usually has a multilayer array structure with two types of alternating surfaces: one side is SiO_6 macro ring, and the other side is $Al(OH)_3$. The negatively charged kaolinite surface is balanced by cations that can be easily exchanged with other cations [10].

In Vietnam, many areas have excellent mineral potential, including halloysite minerals. Tubular halloysite minerals commonly exist in weathered layers of pegmatite bodies of the Tan Phuong complex. Thach Khoan area, Phu Tho, is one of the areas where many pegmatite bodies are distributed in this complex. According to published research results on halloysite mineral characteristics in this area, halloysite exists in two forms with fundamentally different properties [11, 12]. Long halloysite has a more significant tube length (from 750 to 1,250 nm) and is mainly distributed in the lower weathering layer. Short halloysite has shorter tube lengths (from 250 to 750 nm) spread primarily in the upper weathered layer. The surface area of halloysites in the upper layer sample was determined to be 15.7434 $m^2.g^{-1}$; in the lower layer, it was 22.0211 $m^2.g^{-1}$. The inner diameter of halloysite tubes is mainly distributed at 4.3 nm, with smaller diameters of 9.2, 10.7, and 13.5 nm. In addition, the phase composition of the mineral sample shows the simultaneous existence of halloysite, kaolinite, and quartz phases. This study surveyed and evaluated the characteristic properties and ability to recover the rare earth element Ce^{3+} in the water environment of halloysite minerals in the Thach Khoan area, Phu Tho.

II. EXPERIMENTS

2.1. Materials and sample

The halloysite powder was taken after the screening process from Lang Dong Kaolin mine, Thach Khoan, Phu Tho. The samples were mixed well and separated using a wet sieve method with a mesh size of 32 µm. The sample under the sieve was filtered and dried at 60°C. After drying, the sample was tested and analyzed in the following steps.

2.2. Characterization

The material samples' infrared (IR) spectra were recorded using an FT-IR spectrometer (Brucker, Germany) in the 400-4000 cm^{-1} range. Scanning electron microscopy (SEM; Hitachi S-4600, Japan) was used to image the materials' surface and morphologies. Powder X-ray diffraction (XRD) patterns were measured using an X'Pert Pro diffractometer (Jeol, Japan) with CuK_α radiation (15 mA and 40 kV) at a scan rate of 2°.min^{-1} with a step size of 0.02°. The specific surface area values of the halloysite were calculated by the Brunauer Emmett Teller (BET) method and the Langmuir method using the nitrogen adsorption isotherm.

2.3. Adsorption experiments

A series of experiments were conducted at room temperature. The adsorption process was done by mixing an amount of halloysite with 50 mL of Ce^{3+} solution at self-generated pH (~ 6.5). At the reserved times, the remaining Ce^{3+} solution was analyzed, and its residual concentration at equilibration time t (min), (C_e, in $mg.L^{-1}$) was determined by Inductively Coupled Plasma Mass Spectrometry (ICP/MS).

C_o (initial concentration of Ce^{3+}) and C_e values were used to estimate the amount of Ce^{3+} adsorbed on the halloysite at each equilibrium, q_e ($mg.g^{-1}$), was determined as the following equation [13]:

$$q_e = \frac{C_0 - C_e}{m_{hal}} \times V_{Ce^{3+}} \quad (1)$$

where m_{hal} is the halloysite mass (g), and V_{Ce3+} is the volume of the Ce^{3+} solution (L).

Different equilibrium isotherms and adsorption kinetic models were used to study the adsorption process. Excel software employed the linear curve fitting method to fit kinetic and isotherm models to the experimental data. To assure the sureness of results, each investigation was performed three times and averaged.

The Langmuir, Freundlich and Temkin models were used in this study to describe the adsorption equilibrium:

Langmuir equation [13]: $\frac{C_e}{q_e} = \frac{1}{q_m} C_e + \frac{1}{K_L . q_m}$ (2)

Freundlich equation [13]: $lnq_e = lnK_F + \frac{1}{n} lnC_e$ (3)

Temkin equation [14]: $q_e = BlnA + BlnC_e$ (4)

where q_e is the adsorption capacity at equilibrium ($mg.g^{-1}$), q_m is the maximum adsorption capacity of the adsorbent ($mg.g^{-1}$), K_L is Langmuir constant; C_e is the adsorbate concentration at equilibrium (mg/m^3). K_F and n are model constants, K_F is related to the adsorption affinity of the adsorbent, and n indicates the adsorption process's support. B = RT/b, b ($J.mol^{-1}$) is the Temkin constant, related to the heat of adsorption, R (8.314 $J.mol^{-1}.K^{-1}$) is the gas constant, T (K) is the absolute temperature; A is the Temkin thermal constant ($L.g^{-1}$).

The adsorption kinetics of Ce^{3+} were explored based on two models: pseudo-first-order and pseudo-second-order. The kinetic rate constants were calculated, respectively [13].

- The pseudo-first-order equation can be expressed as follows:

$$\ln(q_m - q_t) = lnq_m - k_1 \times \frac{t}{2.303} \quad (5)$$

where q_t and q_m are the adsorbed amounts ($mg.g^{-1}$) at time t (min), and at equilibrium, k_1 (min^{-1}) is the corresponding adsorption rate constant.

- The pseudo-second-order model, as shown below, has been applied broadly for solute adsorption and catalysis reactions in liquid conditions:

$$\frac{t}{q_t} = \frac{1}{k_2 \times q_e^2} + \frac{t}{q_e} \quad (6)$$

where q_t and q_e are the adsorbed amounts ($mg.g^{-1}$) at time t (min), and at equilibrium, k_2 ($g.mg^{-1}.min^{-1}$) is the corresponding rate constant.

III. RESULT AND DISCUSSION

3.1. Characterization

XRD pattern of the halloysite sample in natural is presented in Fig. 1. The results indicated that minerals of the kaolin system coexisted in the material. The characteristic peaks of halloysite - 7 angstroms at the angular positions 19.9°, 24.8°, 35.0°, and 38.4° correspond to the triclinic structure $Al_2Si_2O_5(OH)_4$ (PDF No. 00-29- 1487). The peaks at the angular positions 26.6°, 54.8°, and 62.3° correspond to the hexagonal structure $Al_2Si_2O_5(OH)_4.2H_2O$ (PDF No. 00-29-1489) representing halloysite - 10 angstrom. In addition, the diffraction peaks at angles 12.3°, 22.8° and 45.5° are assigned to the monoclinic structure $Na_{0.3}Al_4Si_6O_{15}(OH)_6.4H_2O$ of kaolinite (PDF-00-029-1490).

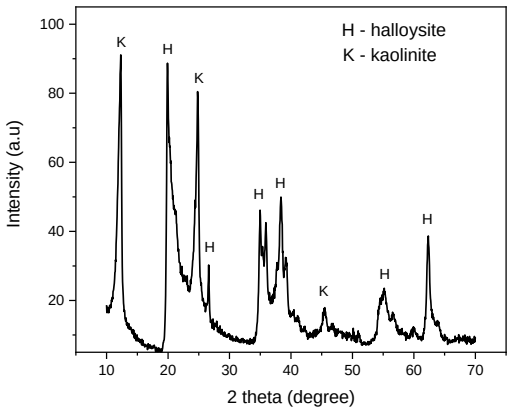

Fig. 1: The XRD patterns of the halloysite

Figure 2 shows the halloysite sample's FT-IR spectra and presents the kaolin minerals' existence. The absorption bands at 3695 and 3621 cm^{-1} in the FTIR spectra are assigned to the stretching vibration due to the inner surface of the O-H groups. The absorption at 1635 cm^{-1} is given to the interlayer water [15]. The Si-O stretching region comprises an absorption band at 1037 cm^{-1}. The band at 914 cm^{-1} is given to the bending vibration of Al-OH. The band observed at 752 cm^{-1} of the sample is set to the stretching mode of Al-O-OH. The low stretching band Si-O defined at 694 cm^{-1} confirms the halloysite in the sample. The band at 539 cm^{-1} is due to the vibration of Al-O-Si [16].

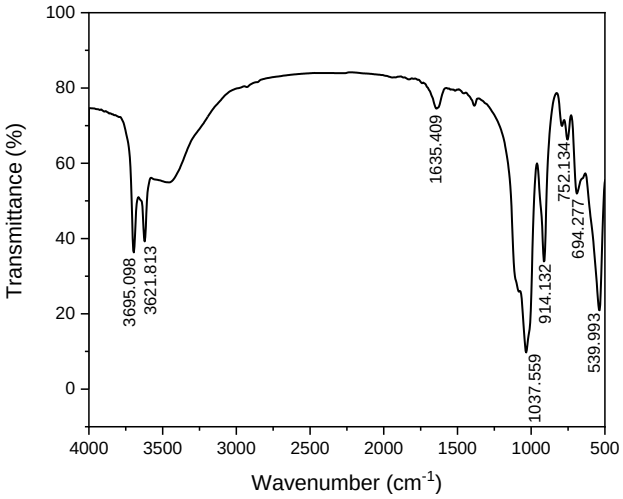

Fig. 2: The FTIR spectroscopy of the halloysite

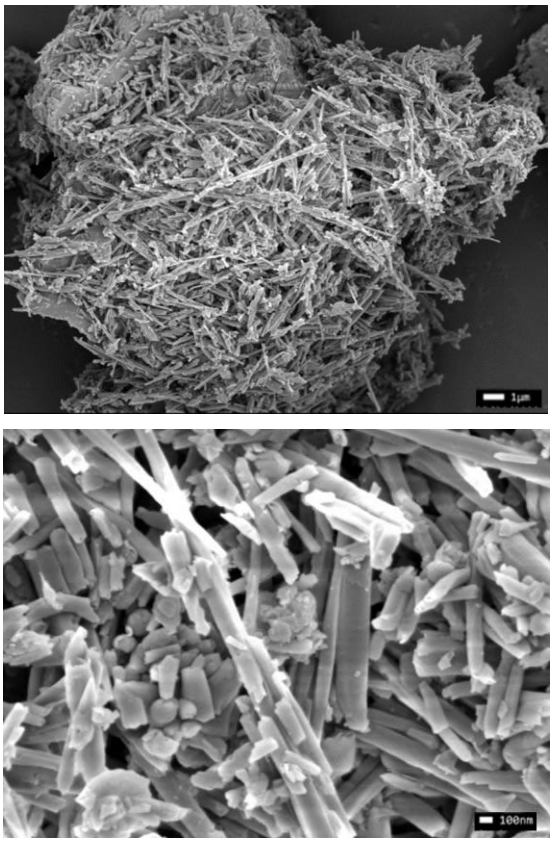

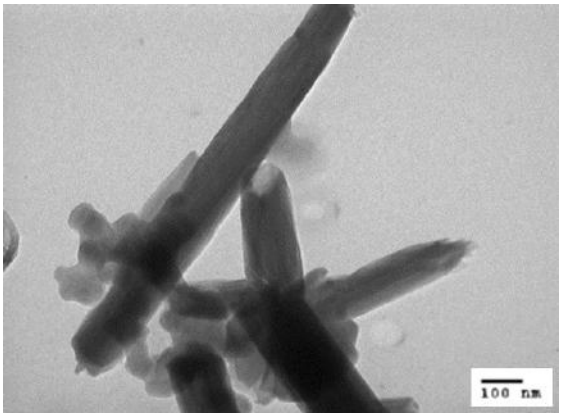

Fig. 3: The SEM (a, b) and TEM (c) images of the halloysite

The SEM images of the samples with the size fraction < 2 µm are shown in Fig. 3a,b. The rod-shaped minerals were interwoven and overlapped each other as matrices. From these images, it can be seen that there may be two types of halloysite available in the samples: short halloysites and long halloysites of the weathered pegmatite profile. The TEM in Fig. 3c also displays the 1D nano morphology of the material.

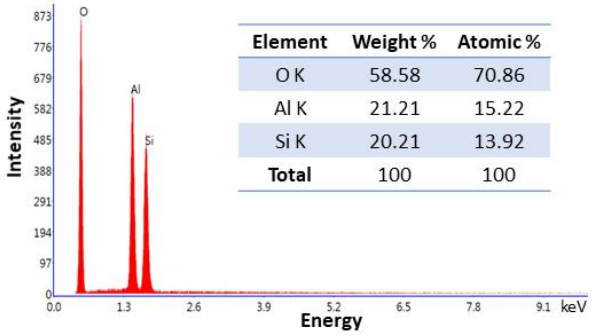

Element	Weight %	Atomic %
O K	58.58	70.86
Al K	21.21	15.22
Si K	20.21	13.92
Total	100	100

Fig. 4: The EDS spectroscopy of the halloysite

The EDS spectra (Fig. 4) shows the main elements of Al, Si, and O relative to the halloysite chemical formula ($Al_2Si_2O_5(OH)_4.2H_2O$).

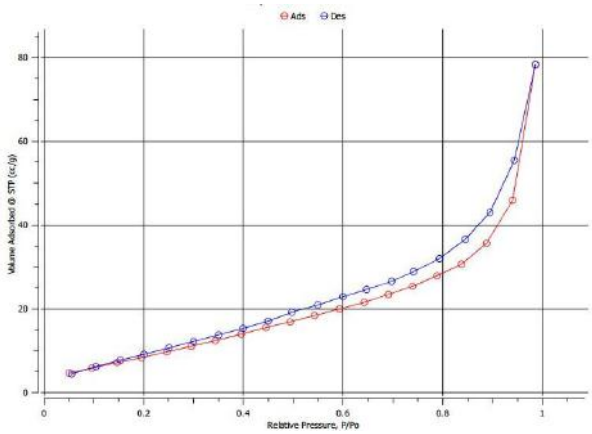

Fig. 5: The BET isotherm plot of the halloysite

The porous property of halloysite was identified by measurement of surface area (BET), which was investigated using N_2 adsorption-desorption isotherms. Nitrogen adsorption isotherms show type I curves, which reveal the microporous nature. The BET surface area of the halloysite in Fig. 5 was 30.93 $m^2.g^{-1}$. With this characteristic, halloysite can adsorb various objects, such as gases [17], toxic organic compounds [18], or heavy metal ions in water [19]. This study tested the halloysite for the adsorption of the ion Ce^{3+} in an aqueous medium.

3.2. Adsorption study

The ability to adsorb Ce^{3+} in halloysite was investigated under the following conditions: the mass of halloysite powder used was 0.5 g/50 mL of Ce^{3+} solution with a concentration of 40 $mg.L^{-1}$ and a pH of 6.5 (initial pH), 25°C. The survey results are shown in Fig. 6. The results show that halloysite has a good adsorption capacity for Ce^{3+}. The adsorption efficiency gradually increases and is almost stable after 60 minutes. After an adsorption time of 60 minutes, the adsorption capacity reaches 2.46 $mg.g^{-1}$ and remaines practically tough as the adsorption time continues to increase.

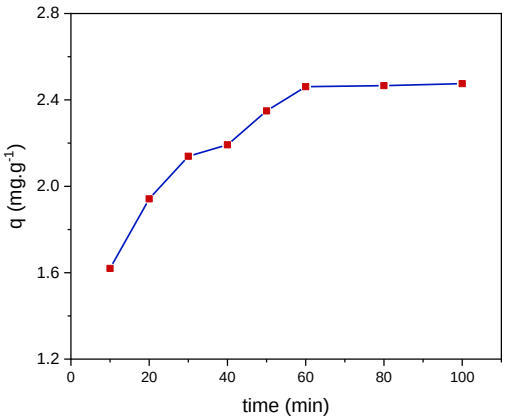

Fig. 6: The Ce^{3+} adsorption capacity of the halloysite

Based on the results of research on the effect of adsorption time on Ce^{3+} adsorption capacity, graphs of pseudo-first-order and pseudo-second-order adsorption kinetic equations can be built, the results are shown in Fig. 7. The results of calculating the value of the adsorption rate constant (k) and the adsorption capacity at equilibrium (q_e) based on the graph obtained in Figure 7 are introduced in Table 1. The pseudo-first-order adsorption kinetics (1.923 $mg.g^{-1}$) differs more from the q_e value determined from experiment (2.48 $mg.g^{-1}$) than the q_e value calculated by the second-order pseudo-adsorption kinetics equation (2.673 $mg.g^{-1}$), at the same time, the regression coefficient of the pseudo-second-order kinetic equation reaches R^2 = 0.9985 ≈ 1 while the regression coefficient of the pseudo-first-order

kinetic equation (0.9359) is far from 1. This result proves that the adsorption process of Ce^{3+} by halloysite follows the pseudo-second-order adsorption kinetic equation. The determined adsorption rate constant is 0.0525 $g.mg^{-1}.min$.

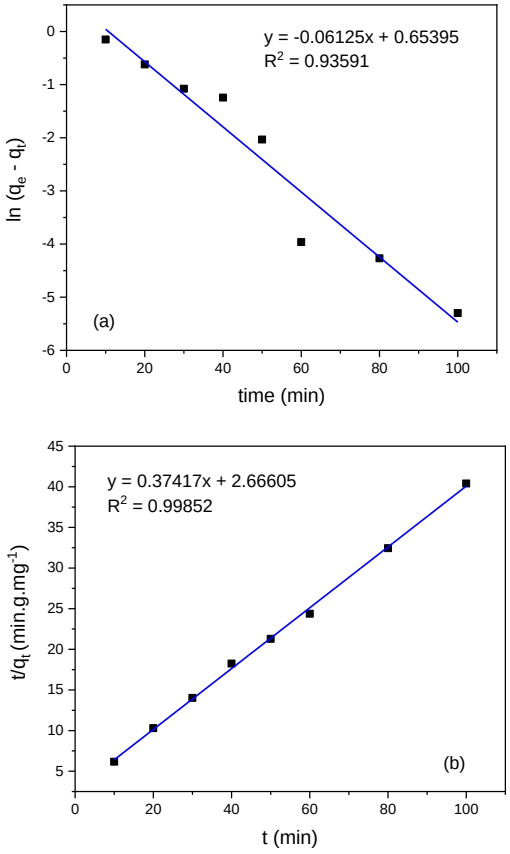

Fig. 7: The pseudo-first-order and pseudo-second-order kinetic curves for Ce^{3+}

Table.1: Isotherm constants and correlation coefficients for the adsorption of Ce^{3+} on halloysite

Pseudo-first-order			Pseudo-second-order			q_e exp (mg. g^{-1})
q_e (mg. g^{-1})	k_1 (min^{-1})	R^2	q_e (mg. g^{-1})	k_2 (g.mg^{-1}.min)	R^2	
1.923	0.06125	0.9359	2.673	0.0525	0.9985	2.48

The pH of the solution is an important factor that affects the adsorption of metal ions in aqueous media. pH not only affects the existence of ionic species in solution but also affects the surface state of the adsorbent [18]. The effect of pH on the Ce^{3+} adsorption capacity of halloysite was investigated in the range from 3.5 ÷ 7.2. The investigated pH range veries around the pH_{PZC} value (zero charge point) of halloysite (pH_{PZC} = 5.99) [19], while ensuring that there is no formation of hydroxide precipitate of Ce^{3+}, thus accurately determine the adsorption efficiency of halloysite to Ce(III) [20]. Investigation experiments were conducted with 0.5 g halloysite/50 mL of Ce^{3+} solution 40 $mg.L^{-1}$, 60 minute adsorption time. The results (Table 2) show that, in the investigated pH range, when pH increases, the adsorption efficiency and capacity increase. This result is explained by the fact that in an acidic environment, halloysite is protonated, then the surface of the particle will be positively charged, leading to a reduction in the number of adsorption centers of halloysite. In addition, the competitive adsorption between H^+ ions and Ce^{3+} ions will reduce the ability to adsorb Ce^{3+} ions [10]. As pH increases, the positive charge density of the surface gradually decreases, the Ce(III) adsorption capacity will gradually increase. pH > pH_{PZC} will be favorable for Ce(III) adsorption. Althought at pH = 6.5 (initial pH), the adsorption efficiency and capacity (61.53% and 2.46 mg/g, respectively) are lower than the values at pH 7.2, but to facilitate the treatment of large quantities without having to adjust pH, pH = 6.5 was chosen for the Ce^{3+} adsorption process in subsequent studies.

Table.2: The effect of pH on the Ce^{3+} adsorption capacity of halloysite

pH	C_{ion}, $mg.L^{-1}$	H, %	q, $mg.g^{-1}$
3.5	27.80	30.51	1.22
4.5	21.45	46.38	1.86
5.5	16.81	57.97	2.32
6.5	15.39	61.53	2.46
6.9	10.41	73.97	2.96
7.2	6.50	83.75	3.35

The effect of halloysite mass on the ability to adsorb Ce^{3+} was studied in the range of 0.3-1.2 g halloysite/50 mL of solution Ce^{3+} 40 $mg.L^{-1}$ at pH 6.5, 25ºC. As the amount of solid adsorbent in the solution increases, the adsorption efficiency increases due to the increase of contact area between the adsorbent and the solution, so there are more active centers for adsorption [18]. According to the results in Table 3, the adsorption efficiency increases greatly from 45.4% to 71.3% as the halloysite mass increases from 0.3 g to 0.8 g, then increases slightly and stabilizes as the amount of adsorbent increases to 1.0 g. However, the adsorption efficiency remains almost unchanged while the adsorption capacity gradually decreases as the mass of the material keeps increasing, because the adsorption reaches an equilibrium state. The ratio of 0.8 g halloysite/50 mL of solution Ce^{3+} 40 $mg.L^{-1}$ giving relatively high adsorption efficiency and capacity is suitable for further research.

Table.3: The effect of halloysite mass on the Ce^{3+} adsorption capacity

m_{hal}, g	C_{ion}, mg.L^{-1}	H, %	q, mg.g^{-1}
0.3	23.99	40.02	2.67
0.5	15.39	61.53	2.46
0.7	11.83	70.43	2.01
0.8	8.41	78.97	1.97
0.9	7.02	82.45	1.83
1.0	6.42	83.96	1.68
1.1	5.46	86.36	1.57
1.2	4.87	87.83	1.46

The initial Ce^{3+} ion concentration has a significant influence on the adsorption capacity and efficiency. In the initial Ce^{3+} concentration range investigated (10 mg.L^{-1}–80 mg.L^{-1}) under the conditions: halloysite mass 0.8 g/50 mL Ce^{3+} solution, pH = 6.5 and room temperature, as the Ce^{3+} concentration increases, the adsorption capacity gradually increases while the adsorption efficiency decreases (Fig. 8). When the initial Ce^{3+} ion concentration is low, the contact area between the Ce^{3+} solution and the halloysite solid phase is large, and the ability to adsorb Ce^{3+} ions onto the halloysite is favorable. However, when the solution concentration increases, the amount of Ce^{3+} ions increases, but the adsorption capacity of halloysite is saturated and does not increase anymore, so the adsorption efficiency will decrease [10]. At a Ce^{3+} concentration of 30 mg.L^{-1}, the adsorption capacity and efficiency reached 1.62 mg.g^{-1} and 86.64%, respectively. This result shows the high adsorption efficiency of halloysite to Ce^{3+} comparable to Cd(II) - 86.31% [19], As(III) - 82.4% [10].

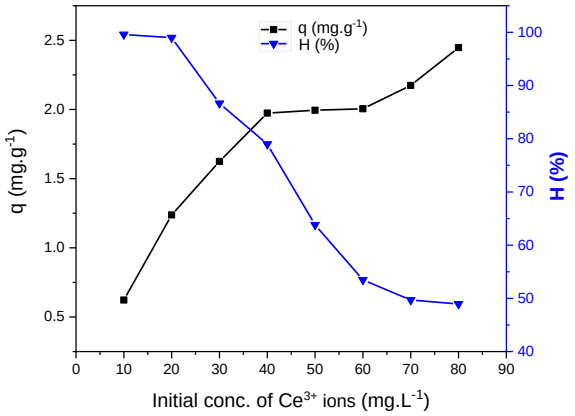

Fig. 8: The effect of initial Ce^{3+} ion concentration on the adsorption capacity

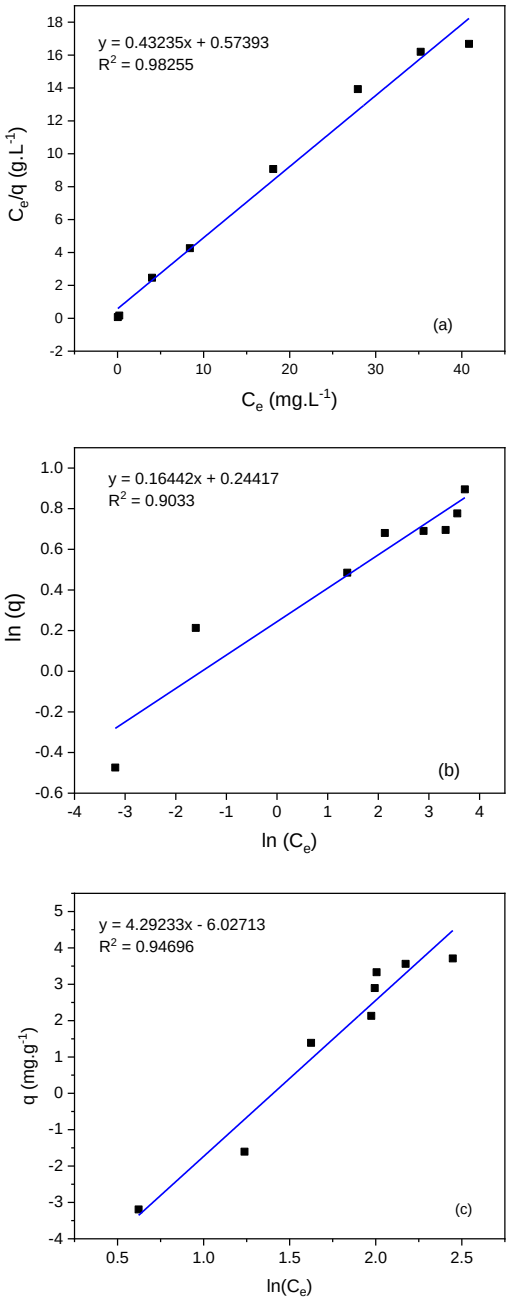

Fig. 9: The adsorption isotherms of Ce^{3+} on halloysite

Table.4: The adsorption isotherms parameters of Ce^{3+} on halloysite

Langmuir	q_m (mg.g^{-1})	2.313
	K_L (L.mg^{-1})	0.753
	R^2	0.98255
Freundlich	K_F (mg$^{1-1/n}$.g^{-1}.L$^{1/n}$)	1.276
	n	6.082
	R^2	0.90330
Temkin	A (L.g^{-1})	0.2456
	B	4.29233

	b (J.mol^{-1})	577.209
	R^2	0.94696

Based on the experimental results of the effect of initial Ce^{3+} ion concentration on the halloysite's adsorption capacity of Ce^{3+}, the linear regression lines between C_e/q_e and C_e (Langmuir model, Fig. 9a), between lnC_e and lnq_e (Freundlich model, Fig. 9b) and between lnC_e and q_e (Temkin model, Fig. 9c) are build. The parameter values of the isothermal equations and other related parameters can be calculated from the slope and intercept values of the vertical axis according to equations (2)-(4), respectively. The results are presented in Table 4.

The results in Fig. 9 and Table 4 show that the Langmuir model is the most suitable among the three models when comparing the reliability coefficient R^2 (the reliability coefficient R^2 of the Langmuir isotherm model is 0.98255, the highest of the three models and close to unity) demonstrating the monolayer physical adsorption. This result is also consistent with studies on the adsorption of halloysite to some other metal ions [21].

IV. CONCLUSION

Halloysite is pretreated with a simple chemical process to create rare earth metal ion adsorbent materials, aiming to recover these elements. The morphology of the pretreated halloysite is rod-shaped and one-dimensional in nano dimensions. The adsorbent material exists in the two-phase form of halloysite-kaolinite. Research results show the high adsorption capacity of halloysite for Ce^{3+}. The Ce^{3+} adsorption process by halloysite follows the pseudo-second-order adsorption kinetic equation and the monolayer physical adsorption model.

ACKNOWLEDGMENTS

This research is sponsored by the project of Hanoi University of Mining and Geology (Project code: T23-14).

REFERENCES

[1] Jha, M. K., Kumari, A., Panda, R., Kumar, J. R., Yoo, K., Lee, J. Y. (2016). Review on hydrometallurgical recovery of rare earth metals. *Hydrometallurgy, 165*(1), 2-26. doi:10.1016/j.hydromet.2016.01.035

[2] Allahkarami, E., Rezai, B. (2019). Removal of cerium from different aqueous solutions using different adsorbents: A review. *Process Safety and Environmental Protection*, *124*, 345-62. doi:10.1016/j.psep.2019.03.002

[3] Fu M, Xu F, Yan J, Wang C, Fan G, Song G, et al. (2022). Mixed valence state cerium metal organic framework with prominent oxidase-mimicking activity for ascorbic acid detection: Mechanism and performance. *Colloids and Surfaces A: Physicochemical and Engineering Aspects*, *641*. doi: 10.1016/j.colsurfa.2022.128610.

[4] Nhàn, N. T., Long, H. P., An, N. T. T., Hiển, V. Đ., Nhiệm, Đ. N., Thơm, Đ. T., Hùng, P. Đ., Thiêm, P. V., Thanh, C. Đ., Cường, N. H., Tuyến, N. Đ. (2021), Study on preparation of multi-oxide photocatalysts containing CeO_2/La_2O_3 from Vietnamese rare earths to treat ammonium, phosphate and bacterial contamination in To Lich river water. *Vietnam Journal of Catalysis and Adsorption*, *10*(1), 373-381. doi:10.51316/jca.2021.141

[5] Kegl, T., Košak, A., Lobnik, A., Novak, Z., Kralj, A. K., Ban, I. (2020). Adsorption of rare earth metals from wastewater by nanomaterials: A review. *Journal of Hazardous Materials*, 386, 121632. doi:10.1016/j.jhazmat.2019.121632

[6] Yuan, P., Tan, D., Annabi-Bergaya, F. (2015). Properties and applications of halloysite nanotubes: Recent research advances and future prospects. *Applied Clay Science*, *112-113*, 75-93. doi:10.1016/j.clay.2015.05.001

[7] Zhang, Y., Tang, A., Yang, H., Ouyang, J. (2016). Applications and interfaces of halloysite nanocomposites. *Applied Clay Science*, *119*, 8–17. 10.1016/j.matchemphys.2022.126612

[8] Altun, T., Ecevit, H. (2022). Adsorption of malachite green and methyl violet 2B by halloysite nanotube: Batch adsorption experiments and Box-Behnken experimental design. *Materials Chemistry and Physics 291*, 126612. doi:10.1016/j.matchemphys.2022.126612

[9] Guo, C., Chen, W., Yan, S., Chen, Y., Zhao, X., Zhang, P., Ma, W., Yang, A. (2023). Novel zirconia-halloysite nanotube material for arsenite adsorption from water. *Journal of Environmental Chemical Engineering*, *11*, 109181. doi:10.1016/j.jece.2022.109181

[10] Aljohani, N. S., Kavil, Y. N., Al-Farawati, R. K., Alelyani, S. S., Orif, M. I., Yasser A Shaban, Y. A., Al-Mhyawi, S. R., X Aljuhani, E. H., Salam, M. A. (2023), The effective adsorption of arsenic from polluted water using modified Halloysite nanoclay. *Arabian Journal of Chemistry*, *16*, 104652. doi: 10.1016/j.arabjc.2023.104652

[11] Bac, B., Dung, N., Khang, L., Hung, K., Lam, N., An, D., Son, P., Anh, T., Chuong, D., Tinh, B. (2018). Distribution and Characteristics of Nanotubular Halloysites in the Thach Khoan Area, Phu Tho, Vietnam. *Minerals*, *8*(7), 290. doi:10.3390/min8070290

[12] Bac, B. H., Nguyen, H., Thao, N. T. T., Duyen, L. T., Hanh, V. T., Dung, N. T., Khang L. Q., An, D. M. (2021). Performance evaluation of nanotubular halloysites from weathered pegmatites in removing heavy metals from water through novel artificial intelligence-based models and human-based optimization algorithm. *Chemosphere*, *282*, 131012. doi:10.1016/j.chemosphere.2021.131012

[13] Sheha, R.R. (2007). Sorption behaviour of Zn(II) ions on synthesized hydroxyapatite. *Journal of Colloid and Interface Science*, *310*(1), 18-26.

doi:10.1016/j.jcis.2007.01.047

[14] Guo, H., Lin, F., Chen, J., Li, F. and Weng, W. (2015). Metal–organic framework MIL-125(Ti) for efficient adsorptive removal of Rhodamine B from aqueous solution. *Applied Organometallic Chemmítry, 29*, 12-19. doi: 10.1002/aoc.3237.

[15] Frost, R.L., Krist, J., Horvath, E., Kloprogge, J.T. (2000). Rehydration and phase changes of potassium acetate-intercalated halloysite at 298K. *Journal of Colloid Interface Science, 226*, 318–327. doi:10.1006/jcis.2000.6807

[16] Li, Y., Zhang, Y., Zhang, Y.F., Liu, M., Zhang, F., Wang, L. (2017). Thermal behavior analysis of halloysite selected from Inner Mongolia Autonomous region in China. *Journal of Thermal Analysis and Calorimetry. 129*, 1333–1339. doi:10.1007/s10973-017-6324-2

[17] Park, S. Ryu, J., Cho, H. Y., Sohn, D. (2022). Halloysite nanotubes loaded with HKUST-1 for CO_2 adsorption. *Colloids and Surfaces A: Physicochemical and Engineering Aspects, 651*, 129750. doi: 10.1016/j.colsurfa.2022.129750

[18] Abdel-Fadeel, M. A., Aljohani, N. S., Al-Mhyawi, S. R., Halawani, R. F., Aljuhani, E.H., Salam, M. A. (2022). A simple method for removal of toxic dyes such as Brilliant Green and Acid Red from the aquatic environment using Halloysite nanoclay. *Journal of Saudi Chemical Society, 26*, 101475.
doi: 10.1016/j.jscs.2022.101475.

[19] Bắc, B. H., Hạnh, V. T, Duyên, L. T., Thảo, N. T. T., Hùng, K. T., An, Đ. M, Lực, T. T., (2021). Nghiên cứu khả năng xử lý ion Cd^{2+} trong môi trường nước bằng haloysit khu vực Thạch Khoán, Phú Thọ. *Science & Technology Development Journal - Science of The Earth & Environment*, 5(1), 312-322. doi:10.32508/stdjsee.v5i1.551

[20] de Farias, A. B. V., da Costa, T. B., da Silva, M. G. C., Vieira, M. G. A. (2021). Cerium recovery from aqueous solutions by bio/adsorption: A review in a circular economy context. *Journal of Cleaner Production, 326*, 129395.
doi: 10.1016/j.jclepro.2021.129395

[21] Anastopoulos, I., Mittal, A., Usman, M., Mittal, J., Yu, G., Núñez-Delgado, A., Kornaros, M. (2018). A review on halloysite-based adsorbents to remove pollutants in water and wastewater. *Journal of Molecular Liquids, 269*, 855–868. doi: 10.1016/j.molliq.2018.08.104